

Dalton Transactions

Accepted Manuscript



This is an *Accepted Manuscript*, which has been through the Royal Society of Chemistry peer review process and has been accepted for publication.

Accepted Manuscripts are published online shortly after acceptance, before technical editing, formatting and proof reading. Using this free service, authors can make their results available to the community, in citable form, before we publish the edited article. We will replace this *Accepted Manuscript* with the edited and formatted *Advance Article* as soon as it is available.

You can find more information about *Accepted Manuscripts* in the [Information for Authors](#).

Please note that technical editing may introduce minor changes to the text and/or graphics, which may alter content. The journal's standard [Terms & Conditions](#) and the [Ethical guidelines](#) still apply. In no event shall the Royal Society of Chemistry be held responsible for any errors or omissions in this *Accepted Manuscript* or any consequences arising from the use of any information it contains.



Journal Name

ARTICLE

Copper(II) Mixed-Ligand Polypyridyl Complexes with Doxycycline – Structures and Biological Evaluation

Received 00th January 20xx,
Accepted 00th January 20xx

DOI: 10.1039/x0xx00000x

www.rsc.org/

Olufunso O. Abosede,^{a,b,f} Nilima A. Vyas,^a Sushma B. Singh,^a Avinash S. Kumbhar^{*a}, Anup Kate,^a Anupa A. Kumbhar,^a Ayesha Khan,^a Andrea Erxleben,^c Peter Smith,^d Carmen de Kock,^d Frank Hoffman,^e Joshua A. Obaleye^b

Mixed-ligand Cu(II) complexes of the type [Cu(doxycycline)(L)(H₂O)₂](NO₃)₂, where doxycycline = [4-(dimethylamino)-3,5,10,12,12a-pentahydroxy-6-methyl-1,11-dioxo-1,4,4a,5,5a,6,11,12a-octahydro-tetracene-2-carboxamide] and L = 2,2'-bipyridine (bpy, **1**), 1,10-phenanthroline (phen, **2**), dipyrrodo[3,2-d:2',3'-f]quinoxaline (dpq, **3**) and dipyrrodo[3,2-a:2',3'-c]phenazine (dppz, **4**) have been synthesised and characterised by structural, analytical, and spectral methods. The single-crystal X-ray structures of **1** and **2** exhibited two different geometry, distorted square-pyramidal and octahedral respectively as well as different coordination modes of doxycycline. The complexes **2-4** exhibit prominent plasmid DNA cleavage at significantly low concentrations probably by an oxidative mechanism. Matrix Metalloproteinase (MMP-2) inhibition studies revealed that all complexes inhibit MMP-2 similar to doxycycline which is a well-known MMP inhibitor with **3** being the most potent. IC₅₀ values of doxycycline and **1-4** against MCF-7 (human breast cancer) and Hela cell lines were almost equal in which **3** showed highest efficiency (IC₅₀ = 0.46 ± 0.05 μM), being consistent with its increased MMP inhibition potency. Antimalarial activity of these complexes against the chloroquine-sensitive *Plasmodium falciparum* NF54 and chloroquine-resistant *Plasmodium falciparum* Dd2 strains reveal that complex **3** exhibited higher activity than artesunate drug against chloroquine-resistant Dd2 strain.

Introduction

Doxycycline (DOX) is one of the most commonly used semisynthetic tetracycline drug in the treatment of diverse infections such as anthrax, chlamydial, pneumonia, cholera, syphilis, malaria and plague.^{1,2} In addition DOX is also an approved matrix metalloproteinase (MMP) inhibitor and thus has been also extensively investigated for its anti-tumour properties in variety of tumour cell lines including breast, colon, renal, prostate, osteosarcoma and melanoma.³⁻⁸ MMP

expression has been shown to be linked to tumour development and progression in these cell lines.⁹ Though the MMP inhibition mechanism is not elucidated completely, chelation of active zinc site of MMP by DOX has been proposed.⁴ The metal ion chelation, especially with Ca²⁺ and Mg²⁺, strongly influences the bioavailability and pharmacokinetics of doxycycline. It was also substantiated that copper(II) may act as a necessary cofactor for its antibiotic activity.^{10,11}

Considering the importance of metal ions in pharmacology of DOX, copper-tetracycline complexation interactions have long been studied to elucidate structural and biological role of copper in DOX activity, availability and biomolecular interactions.^{12,13} Recently, Pereira-Maia and co-workers have reported ternary copper(II) phenanthroline complex of DOX of the type [Cu(doxycycline)(phen)(H₂O)(ClO₄)](ClO₄).¹⁴ Similar to other metal complexes with drugs which exhibit higher biological activity than the parent free drug, here also the complex is more active than the free ligand and exhibits enhanced DNA cleavage on UV-light exposure.¹⁵ Of the several possible binding sites, they propose that DOX binds to Cu(II) via the amide oxygen and the hydroxyl oxygen at ring A (Figure 1) based on IR and UV-visible studies.

Even though DOX has been used clinically since 1960, a detailed structural studies of its crystal forms, protonation pattern and tautomerism have been recently reported,¹⁶⁻¹⁸

^a Department of Chemistry, Savitribai Phule Pune University, Pune- 411007, India
Email: gskum@chem.unipune.ac.in Fax: (+91)-020-25691728.

^b Department of Chemistry, University of Ilorin, PMB 1515, Ilorin, Electronic

^c School of Chemistry, National University of Ireland, Galway, Ireland

^d Division of Pharmacology, Department of Medicine, University of Cape Town Medical School, Observatory 7925, South Africa

^e Institute of Inorganic and Applied Chemistry, Martin-Luther-King-Platz 6, 20146 Hamburg, Germany

^f Present address[†] Federal University Otuoke, PMB 126, Yenagoa, Bayelsa State, Nigeria

[†] Supplementary Information (ESI) available: Synthetic route for **1-4** (Scheme S1), packing diagram and H-bonding in **2** (Figure S2), UV-Vis spectra of **1-4** (Figure S3), ESI-MS spectra of **1-4** (Figure S4), DNA cleavage by **1-3** (Figure S5), DNA cleavage in the presence of radical scavengers for **2** (Figure S6) and **3** (Figure S7), synthesis and characterization of binary complex [Cu(doxycycline)₂](NO₃)₂ and Table 1 and Table 2 for Antimalarial activity of complexes against CQ-sensitive and resistance *P. falciparum* NF54 strain and Dd2 strain resp., Study of stability of complexes in DMSO, water and 1mM NaCl (Figure S8, S9 and S10). EPR spectra (Figure S11) See DOI: 10.1039/x0xx00000x

wherein the structural features are dominated by resonance-assisted hydrogen bond (RAHB) encompassing the enolate and

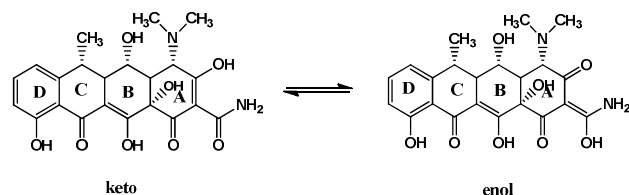
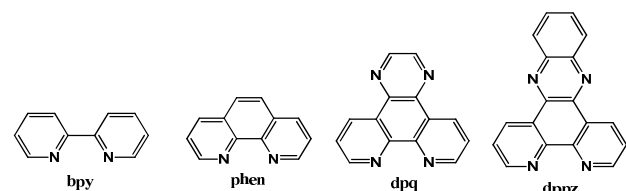


Figure 1. Chemical structure and keto-enol forms of DOX



Scheme 1: Structure of polypyridyl ligands used in the present study

amide atoms based on planarity descriptors and bond lengths.¹⁶ Despite large efforts, the knowledge of structural properties of DOX, in particular protonation-deprotonation equilibria, tautomerism is still unsatisfactory. Contributions related to these structural studies are advantageous for detailed understanding of these properties and in elucidation of chemical biology of DOX. Here, we report single crystal X-ray structures of Cu(II) complexes of DOX where DOX binds to Cu(II) through enolate and diketoamide form of ring A (Figure 1). As far as we are aware of, these are the first single crystal X-ray structures of metal polypyridyl complexes with doxycycline. In the present work mixed-ligand copper(II) complexes, viz $[Cu(\text{doxycycline})(\text{bpy})(\text{H}_2\text{O})]\text{NO}_3$ (**1**), $[Cu(\text{Hdoxycycline})(\text{phen})(\text{H}_2\text{O})_2](\text{NO}_3)_2$ (**2**), $[Cu(\text{Hdoxycycline})(\text{dpq})(\text{H}_2\text{O})_2](\text{NO}_3)_2$ (**3**) and $[Cu(\text{Hdoxycycline})(\text{dppz})(\text{H}_2\text{O})_2](\text{NO}_3)_2$ (**4**) where doxycycline = [4-(dimethylamino)-3,5,10,12,12a-pentahydroxy-6-methyl-1,11-dioxo-1,4,4a,5,5a,6,11,12a-octahydrotetracene-2-carboxamide], bpy = 2,2'-bipyridine, phen = 1,10-phenanthroline, dpq = dipyrido[3,2-d:2',3'-f]quinoxaline and dppz = dipyrido[3,2-a:2',3'-c]phenazine (Scheme 1), have been synthesised and characterised. DNA cleavage, MMP-2 inhibition, cytotoxicity and antimalarial activity of these complexes have been evaluated. The compounds exhibit significant biological potential in terms of their MMP inhibition, cytotoxicity and antimalarial activity.

Experimental section

Reagents and materials: All reagents and solvents were purchased commercially and were used as received. Copper(II) nitrate trihydrate, 2,2'-bipyridine, 1,10-phenanthroline monohydrate and tris(hydroxymethyl) aminomethane (Tris buffer) were purchased from S. D. Fine chemicals (India). Doxycycline hyclate was obtained from Neimeth International Pharmaceuticals Plc, Nigeria. Calf thymus DNA was purchased from SRL (India), supercoiled plasmid pBR322 DNA was

obtained from Bangalore Genei (Bangalore, India). All other chemicals and reagents were of analytical grade and used without further purification.

The ligands 1,10-phenanthroline-5,6-dione (phen), dipyrido[3,2-d:2',3'-f]quinoxaline (dpq) and dipyrido[3,2-a:2',3'-c]phenazine (dppz) were synthesized according to literature protocols.¹⁹⁻²¹

Preparation of Complexes. $[Cu(\text{doxycycline})(\text{bpy})(\text{H}_2\text{O})]\text{NO}_3$ (**1**). 0.121 g (0.5 mmol) $\text{Cu}(\text{NO}_3)_2 \cdot 3\text{H}_2\text{O}$ and 0.256 g (0.5 mmol) doxycycline hyclate were stirred at room temperature for 30 min in 15 mL water-methanol (3:1) after which 0.0781 g (0.5 mmol) 2,2'-bipyridine was added. After additional 4 h of stirring, the resulting blue solution was allowed to evaporate slowly at room temperature. Blue crystalline solid formed after one week was filtered and washed with water and dried in vacuum desiccator over calcium chloride. Yield: 0.305 g, 74%. FT-IR (KBr pellet, ν cm^{-1}): 3356(H_2O), 3078(ArH), 2889, 2775(CH_2), 1608(C=O), 1577, 1454(C=C, C=N), 594, 520(Cu-N, Cu-O). Elem. Anal. Calc. (%) for $\text{C}_{22}\text{H}_{33}\text{N}_5\text{O}_{12}\text{Cu} \cdot \text{CH}_3\text{OH}$: C, 46.13; H, 4.80; N, 9.32. Found: C, 46.02; H, 4.98; N, 9.38. ESI-MS (m/z positive mode), Calc. $[\text{M}-\text{H}_2\text{O}-\text{NO}_3]^+$ 664.15, Found: $[\text{M}-\text{H}_2\text{O}-\text{NO}_3]^+$ 664.1.

$[Cu(\text{Hdoxycycline})(\text{phen})(\text{H}_2\text{O})_2](\text{NO}_3)_2$ (**2**). The complex was prepared using a procedure similar to that for **1** by using 1, 10-phenanthroline instead of 2,2'-bipyridine. Yield: 0.254 g, 65%. FT-IR (KBr pellet, ν cm^{-1}): 3375(H_2O), 3059(ArH), 2823, 2752(CH_2), 1608(C=O), 1577, 1454(C=C, C=N), 513, 455(Cu-N, Cu-O). Elem. Anal. Calc. (%) for $\text{C}_{34}\text{H}_{36}\text{N}_6\text{O}_{16}\text{Cu} \cdot \text{CH}_3\text{OH}$: C, 47.75; H, 4.58; N, 9.04. Found: C, 47.99; H, 4.53; N, 9.12. ESI-MS (m/z positive mode) Calc. $[\text{M}-2\text{H}_2\text{O}-2\text{NO}_3]^{2+}$ 344.09, Found: $[\text{M}-2\text{H}_2\text{O}-2\text{NO}_3]^{2+}$ 343.9.

$[Cu(\text{Hdoxycycline})(\text{dpq})(\text{H}_2\text{O})_2](\text{NO}_3)_2$ (**3**). The complex was prepared using a procedure similar to that for **1** by using dipyrido[3,2-d:2',3'-f]quinoxaline instead of 2,2'-bipyridine. Yield: 0.180 g, 41%. FT-IR (KBr pellet, ν cm^{-1}): 3390(H_2O), 3078(Ar-H), 1614(C=O), 1581(Ar-H), 1483(CH_2), 607, 511(Cu-N, Cu-O). Elem. Anal. Calc. (%) for $\text{C}_{36}\text{H}_{36}\text{N}_8\text{O}_{16}\text{Cu} \cdot \text{H}_2\text{O}$: C, 47.1; H, 4.46; N, 12.20. Found: C, 47.44; H, 4.53; N, 12.37. ESI-MS (m/z positive mode) Calc. $[\text{M}-2\text{H}_2\text{O}-2\text{NO}_3]^{2+}$ 740.2, Found: $[\text{M}-2\text{H}_2\text{O}-2\text{NO}_3]^{2+}$ 738.5.

$[Cu(\text{Hdoxycycline})(\text{dppz})(\text{H}_2\text{O})_2](\text{NO}_3)_2$ (**4**). The complex was prepared using a procedure similar to that for **1** by using dipyrido[3,2-a:2',3'-c]phenazine instead of 2,2'-bipyridine. Yield: 0.29 g, 67%. FT-IR (KBr pellet, ν cm^{-1}): 3371(H_2O), 3078(Ar-H), 1612(C=O), 1585, 1496(C=C, C=N). Elem. Anal. Calc. (%) for $\text{C}_{40}\text{H}_{38}\text{N}_8\text{O}_{16}\text{Cu}$: C, 51.55; H, 3.76; N, 11.79. Found: C, 51.60; H, 3.86; N, 11.77. ESI-MS (m/z positive mode) Calc. $[\text{M}-2\text{H}_2\text{O}-2\text{NO}_3]^{2+}$ 790.286, Found: $[\text{M}-2\text{H}_2\text{O}-2\text{NO}_3]^{2+}$ 790.1.

Physical Methods

FT-IR spectra were recorded as KBr pellets on a Shimadzu FTIR-8400 spectrophotometer. Electronic absorption spectra were recorded on a Jasco UV-vis spectrophotometer (V-630) in the range of 200-900 nm using a matched pair of 1 cm quartz cells.

The electron spin resonance (ESR) spectra were recorded in DMSO at 77 K on E-112 ESR spectrometer, VARIAN USA at Sophisticated Analytical Instrument Facility, Indian Institute of Technology Bombay, Powai, Mumbai, India. The electrospray mass spectra were recorded on a MICROMASS QUATTRO II triple quadrupole mass spectrometer. Microanalyses (C, H, and N) were carried out with a ThermoQuest microanalysis instrument capable of carrying out CHNS (carbon, hydrogen, nitrogen, and sulfur) analyses.

Single-crystal X-ray diffraction studies. The single-crystal X-ray diffraction data for **1** was collected at 100 K using Mo-K α radiation. The structures were solved by direct methods and subsequent Fourier syntheses and refined by full-matrix least squares on F^2 using SHELXS-2013 and SHELXL-2013 as integrated in the SHELXTL 2013 suite.²² All non-hydrogen atoms of **1** were refined anisotropically. Hydrogen atoms, except those of the hydroxyl groups at the ring system and of the coordinated water molecule at the Cu(II) site, were generated geometrically and refined as riding atoms with isotropic displacement factors equivalent to 1.2 times those of the atom to which they were attached (1.5 for methyl groups). The absolute structure was determined and is in agreement with the selected setting (Flack parameter: 0.085(23)).²³ CCDC no. of **1** is 1048414

The single-crystal diffraction data for **2** was collected with an Oxford Diffraction Xcalibur CCD at room temperature using Mo-K α radiation. The structures were solved by direct methods and subsequent Fourier syntheses and refined by full-matrix least squares on F^2 using SHELXS-97, SHELXL-97^{24,25} and Oscal.²⁶ All non-hydrogen atoms of **2** were refined anisotropically. Hydrogen atoms, except those for the water molecules of crystallization, were generated geometrically and refined as riding atoms with isotropic displacement factors equivalent to 1.2 times those of the atom to which they were attached (1.5 for methyl groups). Graphics were produced with XP in SHELXTL-PC and ORTEX.²⁷ The absolute structure for **2** was determined and is in agreement with the selected setting (Flack parameter: 0.07(5)).²³ CCDC no. of **2** is 987897.

Biological evaluation.

The test samples were prepared as stock solution in 100% dimethyl sulfoxide (DMSO) and were stored at -20 °C. Further dilutions were prepared on the day of the experiment as required. There is no change in the UV-Visible spectrum of the complexes in DMSO, water and 1mM NaCl solution evidencing stability and integrity of complexes in solution.

DNA cleavage experiments. For the gel electrophoresis experiments, supercoiled pBR322 DNA (300 ng in nucleotide) was treated with various concentration of metal complexes in TBE buffer (Tris-boric acid-ethylenediaminetetraacetic acid) containing < 5% DMSO and the mixture was incubated for 30 min at 37 °C. The samples were analyzed by 1% agarose gel electrophoresis TBE buffer, pH 8.2 for 3 h at 60 mV. The gel was stained with 0.5 $\mu\text{g mL}^{-1}$ ethidium bromide, visualised by UV light, and photographed for analysis. The extent of cleavage of the SC DNA was determined by measuring the

intensities of the bands using the Alpha Innotech Gel Documentation System (Alphamager 2200). For mechanistic investigations, experiments were carried out in the presence of radical scavenging agents, viz., DMSO, mannitol, diazabicyclo-[2,2,2]-octane (DABCO), NaN₃, L-histidine and SOD (superoxide dismutase enzyme), which were added to supercoiled plasmid pBR322 DNA prior to the addition of the complex. The stock solution of complex was prepared in deionised water containing 5% DMSO.

MMP-2 inhibition studies. Human cervical cancer cell line (HeLa) have been reported to be associated with increased expression of MMP-2 and tumour aggression has been found to significantly correlate with increased levels of MMP-2 and MMP-9 in many experimental and clinical studies.²⁸ A substrate gel zymography of the activity of the MMP-2 of crude proteins from HeLa cell culture supernatants was performed. 500 μL aliquots containing 2.5×10^5 of HeLa cells were added to each of the triplicate wells containing Dulbecco's modified Eagle's medium (DMEM) with 10% foetal bovine serum (FBS). After incubation for 24 h, 15 μM of each of the complexes in phosphate buffer solution (PBS) (in 1% DMSO) were added to the cells in a culture medium without FBS. The supernatant was collected after 48 h incubation. Gelatinase zymography was utilized because of its high sensitivity to gelatinolytic enzymatic activity and ability to detect both pro and active forms of MMP-2. Upon renaturation of the enzyme, the gelatinases digest the gelatin in the gel and reveal clear bands against an intensely stained background. The crude proteins from each sample were mixed with Tris-Glycine SDS Sample Buffer (2X) and resolved on a 10% Zymogram (gelatin) gel in the presence of 0.1% gelatin under non-reducing conditions. Culture media (20 μL) were mixed with sample buffer and loaded for SDS-PAGE (Polyacrylamide gel electrophoresis) with tris glycine SDS buffer. Samples were not boiled before electrophoresis. Following electrophoresis the gels were washed twice in 2.5% Triton X-100 for 30 min at room temperature to remove SDS. The gels were then incubated at 37°C overnight in substrate buffer containing 50 mM Tris-HCl and 10 mM CaCl₂ at pH 8.0 and stained with 0.5% Coomassie Blue R250 in 50% methanol and 10% glacial acetic acid for 30 min and destained. Protein standards were run concurrently and approximate molecular weights were determined by plotting the relative mobilities of known proteins. Gelatinase zymograms were scanned using Alpha imager Gel doc system. The intensity of the bands was evaluated using the pixel-based densitometer program Un-Scan-It, Version 5.1.

Determination of the antiplasmodial activity. Samples of **1-4**, the binary complex [Cu(doxycycline)₂] (NO₃)₂ and doxycycline hyclate were tested in triplicate against chloroquine-sensitive (NF54) and chloroquine-resistant (Dd2) strains of *Plasmodium falciparum*. Continuous *in vitro* cultures of asexual erythrocyte stages of *P. falciparum* were maintained using a modified procedure of Trager and Jensen.²⁹ Quantitative assessment of *in vitro* antiplasmodial activity was determined with the parasite lactate dehydrogenase assay using a modified method of Makler and Hinrichs.³⁰ The test samples were prepared to a

20 mg/mL stock solution in 100% DMSO. Stock solutions were stored at -20°C . Further dilutions were prepared on the day of the experiment. Chloroquine diphosphate (CQDP) and artesunate were used as the reference drugs. A full dose-response experiment was performed for complex **1-4** to determine the concentration inhibiting 50% of parasite growth (IC_{50} -value). Samples were tested at a starting concentration of $100\mu\text{g}/\text{mL}$, which was then serially diluted 2-fold in complete medium to give 10 concentrations; with the lowest concentration being $0.2\mu\text{g}/\text{mL}$. Reference drugs were tested at a starting concentration of $1000\text{ ng}/\text{mL}$. The highest concentration of solvent to which the parasites were exposed to had no measurable effect on the parasite viability (data not shown). The IC_{50} -values were obtained using a non-linear dose response curve fitting analysis via Graph Pad Prism v.4.0 software.

Cytotoxicity studies. Cytotoxicity studies were carried out on a MCF-7 cell line, which was obtained from National Center for Cell Science, Pune University, Pune, India. Cell viability was tested using (3-(4,5-Dimethylthiazol-2-yl)-2,5-diphenyl tetrazolium Bromide (MTT) assay method. The cells were seeded in a 24-well plate at a density of 10^4 cells per well in DMEM containing 10% FBS and a 0.1% antibiotic solution for 24 h at 37°C and 5% CO_2 for adherence. **1-4**, in a concentration of $50\text{--}400\mu\text{g}/\text{mL}$, dissolved in 1% DMSO and PBS buffer, were added to the wells with a fresh medium. 1% DMSO was used as a vehicle control. After every 24, 48, and 72 h of incubation, MTT assay was carried out. A MTT solution ($20\mu\text{L}$, $5\text{ mg}/\text{mL}$) prepared in a 10 mM phosphate buffer was added to each well and incubated for 4 h. The purple formazan product was dissolved by addition of $100\mu\text{L}$ of DMSO for 5 min. The absorbance was measured at 570 and 630 nm (for blank) using an ELISA plate reader, and the viability was calculated. Data were collected for three replicates each and were used to calculate the mean. The percentage inhibition was calculated from this data:

$$\% \text{ inhibition} = \frac{\text{mean OD of untreated cells (control)}}{\text{mean OD of treated cells (control)}} \times 100$$

Results and Discussion

Syntheses and Characterization. Mixed-ligand complexes **1-4** were obtained as their nitrate salts from methanol-water solvent system in good yield (Scheme SI-1). All complexes are partially soluble in water and completely soluble in DMSO and DMF. Complexes were characterized by elemental analysis, UV-vis, IR, electrospray mass spectroscopy and single crystal X-ray structures of **1** and **2** have been determined. Time dependent UV-Vis spectroscopy of complexes in various solvents (DMSO, water and 1 mM NaCl solution) exhibited no changes over the period of 24 hr, indicates that these complexes are stable and retain their structural integrity in solution (Figure S8 - S10 in supporting information)

Crystal structure of 1. Single crystals of **1** were grown by slow evaporation of its solution in methanol: water (1:1). An ORTEP diagram of **1** is depicted in Figure 2. The square pyramidal coordination sphere at the Cu(II) site involves two oxygen

atoms from DOX, two nitrogen atoms of the bipyridyl ligand and one oxygen atom of the axial bound water molecule, which results in a square-pyramidal CuN_2O_3 coordination sphere. The axial Cu-O distance of $2.3926(5)\text{ \AA}$ (Cu-OW1) is longer than the equatorial Cu-O (doxycycline) and Cu-N (bipyridine) distances.

The average equatorial Cu-O bond distance is $1.923(5)\text{ \AA}$, which is shorter than average equatorial Cu-N bond distance,

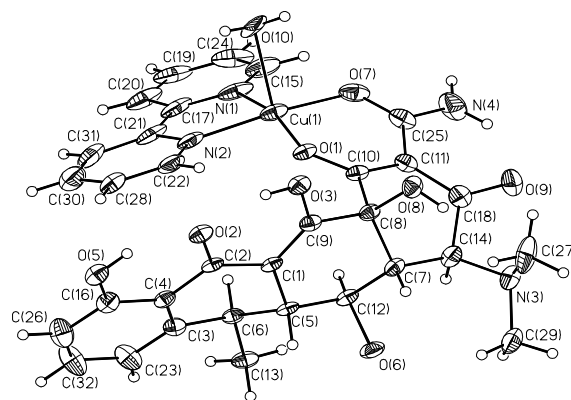


Figure 2. ORTEP diagram of **1** showing atom numbering and thermal ellipsoids drawn at 30% probability. NO_3^- ion is omitted for clarity.

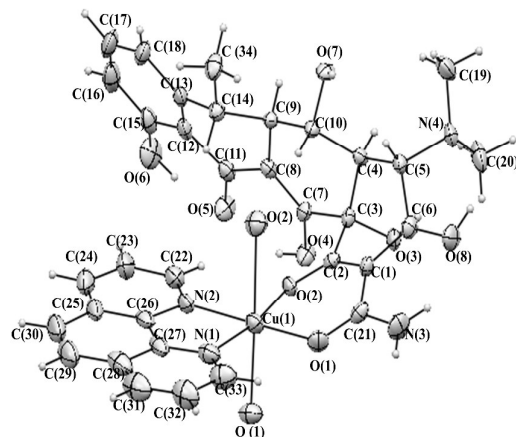


Figure 3. ORTEP diagram of **2** showing the atom numbering scheme and Thermal ellipsoids are drawn at 30% probability. $(\text{NO}_3)^-$ ions are omitted for clarity

which is $1.994(6)\text{ \AA}$. These distances are comparable to those observed in the copper complexes containing two nitrogen and two oxygen atoms coordinated to copper in the basal plane.^{31,32}

Crystal structure of 2. Single crystals of **2** were grown by slow evaporation of its solution in methanol: water system (1:1). The compound crystallizes in the $P2_12_12_1$ space group. An ORTEP representation is shown in Figure 3. **2** exhibits distorted octahedral geometry with a coordination as CuN_2O_4 type and the donor atoms in basal plane are two nitrogen atoms from phenanthroline and two oxygen atoms from doxycycline. Axial sites are occupied by two water molecules with Cu-O distances

of 2.311(4) Å (Cu-Ow1) and 2.559(4) Å (Cu-Ow2), which are longer than the equatorial Cu-O and Cu-N distances. This axial elongation of octahedron is a consequence of tetragonal distortion caused by the Jahn-Teller effect as observed in the octahedral copper complexes.^{33,34} The average equatorial Cu-O bond distance is 1.923(4) Å, which is shorter than average equatorial Cu-N bond distance which is 2.024(5) Å. These distances are comparable to those observed in the copper complexes with two nitrogen and two oxygen atoms coordinated to copper in the basal plane. The coordination geometry at the copper(II) site is a distorted octahedron with bond angles O1-Cu1-N2 = 176.2°, O2-Cu1-N1 = 171.20°, O1w-Cu1-O2w = 178.36°, O2-Cu1-O2W = 86.55°, which deviate slightly from those expected for an ideal octahedral geometry. The planar phenanthroline ligand of one molecule form π - π stacks with the ring D of doxycycline of the neighbouring molecule. Intense intramolecular and intermolecular hydrogen bond networks are formed due to diverse functionalities of doxycycline, nitrate ions, and water molecules stabilizing the structure (Figure S1 and S2 in supporting information).

Table 1: Selected crystallographic data of **1** and **2**

Complex	1	2
Empirical Formula	C ₃₂ H ₃₃ CuN ₅ O ₁₂	C ₃₄ H ₄₁ CuN ₆ O _{19.5}
Formula weight	743.17	900.21
Temperature, K	100	293
Wavelength, Å	0.71073	0.71070
Crystal system, space group	Orthorhombic, <i>P</i> 2 ₁ 2 ₁ 2 ₁	Orthorhombic, <i>P</i> 2 ₁ 2 ₁ 2 ₁
unit cell dimensions	<i>a</i> = 10.2571(7) <i>b</i> = 12.8336(8) <i>c</i> = 28.5532(19)	<i>a</i> = 10.2282(4) <i>b</i> = 12.6403(7) <i>c</i> = 31.3839(16)
Volume, Å ³	3758.62(4)	4057.6(3)
Z, calculated density, g/cm ³	4, 1.313	4, 1.474
F(000)	1540	926
Crystal size, mm ³	0.10 x 0.15 x 0.22	0.20 x 0.30 x 0.35
θ range for data collection, °	2.1-30	3.2-29.1
GOOF on <i>F</i> ²	1.035	1.047
Final R indices [<i>I</i> > 2 σ (<i>I</i>)]	<i>R</i> ₁ = 0.0881, <i>wR</i> ₂ = 0.2015	<i>R</i> ₁ = 0.0632, <i>wR</i> ₂ = 0.1478
R indices (all data)	<i>R</i> ₁ = 0.0721, <i>wR</i> ₂ = 0.1933	<i>R</i> ₁ = 0.0886, <i>wR</i> ₂ = 0.1670

Table 2: Selected Bond Lengths [Å] of **1** and **2**

1			
Cu1-O1	1.925(4)	Cu1-O10W	2.396(5)
Cu1-N3	1.985(6)	Cu1-O2	1.920(5)
Cu1-N4	2.002(6)	C1-O1	1.270(7)
C7-O2	1.269(8)		
2			
Cu1-O1	1.930(4)	Cu1-O2W	2.559(5)
Cu1-O1W	2.311(4)	Cu1-N1	2.024(5)
Cu1-O2	1.917(4)	Cu1-N2	2.024(5)
C2-O2	1.252(6)	C21-O1	1.270(7)

Comparison of structures and binding modes of DOX. The unique structural scaffold of DOX bearing keto-enol functional

groups offer various metal chelation sites. The different possible copper binding sites are shown in figure 4. **1** exhibits square pyramidal geometry with DOX coordination through monoanionic enolate form (iii) whereas **2** exhibits distorted octahedral geometry with the doxycycline coordination through diketoamide group of the ring A (iv). These binding modes of DOX are different than what was proposed earlier^{14,15}, viz. amide oxygen and the hydroxyl oxygen of ring A (ii). The diketoamide coordination in tetracycline was predicted based on the crystal structure investigation of a simple model system bis(*N*-phenyl-2-carbamoyl-5,5'-dimethylcyclohexane-1,3-dionato)copper(II).³⁵ However, as far as we are aware of the present crystal structures of **1** and **2** are the first structures which unequivocally establish the different binding mode of doxycycline in particular and tetracyclines in general.

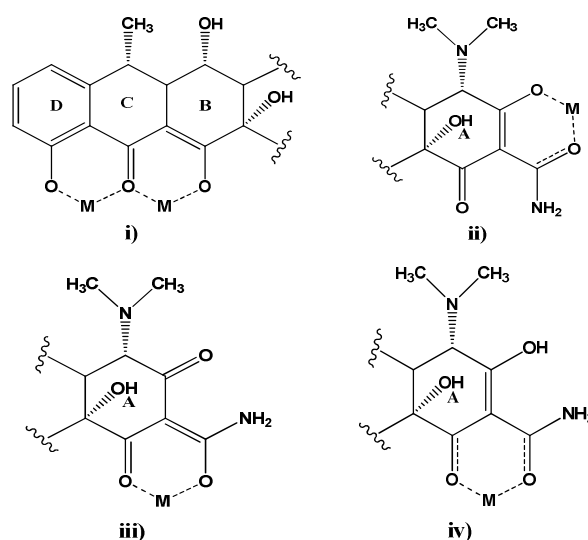


Figure 4. The possible binding sites of doxycycline with copper (i) observed in DOX uptake and biomolecular binding, ref. 11 (ii) predicted in ref. 14 (iii) complex **1**, present work, (iv) complex **2**, present work

UV-Visible and IR spectroscopy. In aqueous solution, the complexes exhibit an intense absorption band in the UV region (250-360 nm) which is attributed to intra-ligand π - π^* transition. The band in the range 360-380 nm has been assigned to charge transfer band. In the visible region (620-640 nm) **1-4** exhibit one very weak broad band of d-d transition. These similar electronic properties show that Cu(II) is in the square coordination geometry and has similar coordination environment in **1-4**. (Table 3) (Figure S3 in supporting information)

Table 3. Spectroscopic data of **1-4** in water at room temperature

Complex	Electronic data $\lambda(\text{nm})/\epsilon(\text{M}^{-1}\text{cm}^{-1})$		
	Ligand Transitions ^a	Charge Transfer ^a	MLCT ^b
1	246/37562	360/20345	628/406
	300/48008		
2	272/52500	360/18259	630/101
	294/29700		
3	256/90000	363/13035	630/97
	292/43035		
4	276/64425	364/19550	637/264
	380/16713		

^a[Complex]= 20 μM , ^b[Complex]= 1 mM

The IR spectrum of the doxycycline ligand shows prominent individual peaks at 1678, 1616 and 1577 cm^{-1} for three carbonyl stretching frequencies ($\nu(\text{C}=\text{O})$) of amide, ring A and ring C, respectively.^{14,36} In the IR spectra of the complexes the $\nu(\text{C}=\text{O})$ of the amide and ring A keto group cannot be distinguished suggesting involvement of these groups in copper binding. The IR bands in the region 530-560 cm^{-1} are assigned to $\nu(\text{Cu}-\text{N})$ coordination in complexes **1-4**. All spectra show $\nu(\text{Cu}-\text{O})$ stretching at $\sim 515\text{-}525 \text{ cm}^{-1}$.

Electron Paramagnetic Resonance

Frozen solution EPR spectra of the complexes exhibit an axial g tensor suggesting square based geometry. Table 4 shows EPR data of the complexes in DMSO at 77K. Complexes **1**, **2** and **3** show well resolved hyperfine features due to Cu(II) nuclei ($I=3/2$) in lower field region and N nuclei hyperfine splitting was barely observed. Complex **4** exhibits low resolved spectrum due to its poor solubility. The trend $g_{\parallel} > g_{\perp} > 2.0023$ for all complexes indicate square based geometry and $d_{x^2-y^2}$ orbital as a ground state of Cu(II).³⁷

Table 4: EPR data of complex **1-4**

Complex	EPR data			
	g_{\parallel}	g_{\perp}	$A_{\parallel}(\text{G})$	$A_{\perp}(\text{G})$
1	2.27	2.08	190	40
2	2.28	2.08	200	40
3	2.33	2.08	187	50
4	2.30	2.08	200	50

Biological Evaluation

DNA Cleavage. The DNA cleavage activities of **1-4** are monitored using supercoiled pBR322 plasmid DNA in the absence of external oxidizing or reducing agents under physiological conditions. **2-4** displayed significant chemical nuclease activity in absence of any external agent (Figure S5 in supporting information). Complex **1** did not show any apparent DNA cleavage at highest concentration tested (100 μM). The DNA cleavage activity follows the order as **4** > **3** > **2**. At 20 μM , **4** convert all supercoiled form of the plasmid to yield nicked circular and linear forms (Figure 5 and Figure 6 C)). The

formation of linear form of DNA by groove binding copper complexes containing aqua/nitrate ligand suitable for intramolecular nucleophilic activation has been reported earlier.^{38,39}

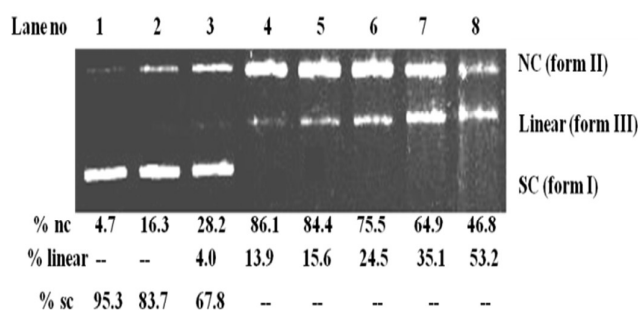


Figure 5. Photographs of 1% Agarose gel showing cleavage of plasmid pBR322 DNA by **4** incubated at 37°C for 20 min. [DNA] = 300 ng. Lane 1, DNA Control; Lanes 2-7, DNA + **4**, 5, 10, 20, 30, 40, 50, 100 μM

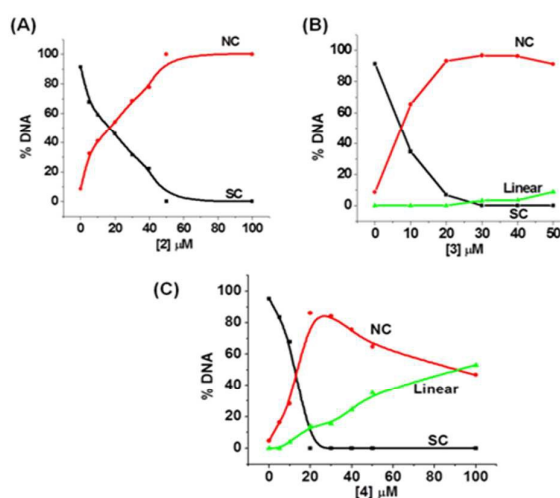


Figure 6. Concentration dependent DNA cleavage by **2-4** (A-C) using plasmid pBR322 DNA of complex (**2-4**) incubated at 37°C for 20 min, [DNA] = 300 ng.

These complexes were incubated with different reactive oxygen species (ROS) inhibitors to investigate the mechanism of DNA cleavage. Hydroxyl radical scavengers (DMSO, mannitol), and superoxide radical scavenger (SOD, superoxide dismutase) showed inhibition of the DNA cleavage activity of **2-4** (**4**; Figure 8: lanes 2, 3) and (**2-3**); Figures S6 and S7) whereas DNA cleavage was not affected by singlet oxygen quenchers DABCO and sodium azide (Figure 8, lanes 4 and 5). Gel photograph of effect of inhibitors on cleavage of pBR322 plasmid DNA by **4** is shown in Figure 7. These results suggest chemical involvement of hydroxyl radicals and superoxide radicals in DNA cleavage. Thus **2-4** cleave DNA by an oxidative mechanism. In all cases we do not observe any drastic shift in electrophoretic mobility^{40,41} which rules out the possibility of covalent binding of the complexes reported for cisplatin and related complexes. The bulky doxycycline ancillary ligand sterically hinders the covalent binding.

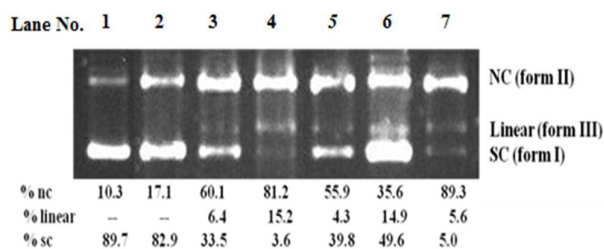


Figure 7. Photograph of 1% agarose gel showing the effect of inhibitors on cleavage of pBR322 plasmid DNA by 4 on incubation for 20 min at 37°C. [DNA] = 300 ng, [4] = 30 μ M; Lane 1, DNA control; lane 2, DNA + 4 + DMSO; lane 3, DNA + 4 + mannitol (50 mM); lane 4, DNA + 4 + DABCO (10 mM); lane 5, DNA + 4 + NaN₃ (20 mM) lane 6, DNA + 4 + SOD (15 units); lane 7, DNA + 4.

MMP-2 Inhibition. Matrix Metalloproteinases are a family of zinc-dependent endopeptidases that are involved in various aspects of cancer phenotype such as cancer oogenesis, invasion/metastasis and angiogenesis and therefore represents a promising target for anticancer drugs.⁶ Ruthenium based complex NAMI-A which has successfully completed phase I clinical trials, is shown to inhibit MMP.^{42,43} Natalie *et al.* have demonstrated that Pt(II) complexes with labile ligands can selectively inhibit MMP by forming hydroxo bridge with catalytic zinc ion of MMP resulting in subsequent loss of MMP activity.⁴⁴ Interestingly the anticancer drugs cisplatin, carboplatin and oxaliplatin with two labile ligands do not inhibit MMP. HeLa cells exhibit a dose-dependent decrease of MMP-2 expression with DOX treatment.^{1,45} Hence, the effects of **1-4** (10 μ M) have been investigated for their MMP-2 expression. Expression of MMP-2 in untreated HeLa cells and treated with **1-4** and doxycycline for 95 h is shown in Figure 8. It is observed that all the complexes except **1** inhibit MMP-2 activity higher than DOX (Figure 8) with **3** being the most potent (relative density of the band = 0.05 \pm 0.001).

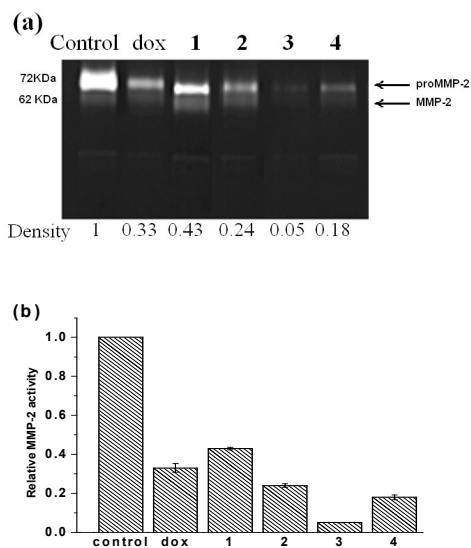


Figure 8. Gelatin zymography for determination of MMP-2 activity in HeLa cells. Results are the mean of three independent experiments carried out under identical conditions

Antimalarial Activity. Among tetracyclines, doxycycline is effectively used in the treatment of malaria especially for chloroquine (CQ) and multidrug-resistant *P. falciparum* malaria.⁴⁶ Studies of antimalarial activity of chloroquine complexes with metals like ruthenium, platinum and gold indicated enhanced activity of complexes more than the parent drug chloroquine and also good activity against chloroquine resistant parasites, suggesting a role of metal in the drug activity.⁴⁷⁻⁵¹ In the present study, activity of **1-4** was evaluated *in vitro* against CQ-sensitive strain NF54 and CQ-resistant strain Dd2 of *P. falciparum* (Table 5).

All complexes exhibit moderate activity than DOX against CQ-sensitive *P. falciparum* NF54 strain but high activity against CQ-resistance Dd2 strain. The complex **3** and **4** are more active than the drug artesunate against CQ-resistance Dd2 strain.

Table 5: Antimalarial activity of complexes against CQ-sensitive and CQ-resistance *P. falciparum* NF54 strain and Dd2 strains

Compound	IC ₅₀ (μ M) ^a	IC ₅₀ (μ M) ^b
1	12.11	4.86
2	2.00	0.85
3	0.35	0.62
4	1.10	0.59
[Cu(dox) ₂]	20.46	6.41
Doxycycline hyclate	19.50	10.87
Chloroquine	0.052	112.63
Diphosphate(CQDP)		
Artesunate	-	9.23

^aIC₅₀ against CQ-sensitive *P. falciparum* NF54 strain, ^bIC₅₀ against CQ-resistance *P. falciparum* Dd2 strain, dox = doxycycline

Cytotoxicity Studies. MTT assay was performed to check cytotoxic effect of doxycycline and **1-4** towards MCF-7 and HeLa cell lines. The cytotoxicity of the DOX and the complexes (**1-4**) were found to be similar in both the cell lines. Cell survival is nearly 50% after 48 h of incubation with doxycycline and complexes (Figure 10). Above 1.5 μ M tested concentration, cells showed necrosis. Doxycycline and all complexes exhibited significant cytotoxic effect with almost similar values of IC₅₀ (0.75 to 0.8 μ M) except for complex **3** exhibiting nearly half IC₅₀ (0.46 μ M) value (Table 6). Cytotoxicity results correlate with the MMP inhibition potential for all complexes suggesting primary involvement of MMP inhibition in cell death along with DNA damage.

Table 6: IC₅₀ values of doxycycline and complexes (**1-4**) towards MCF-7 and HeLa cell line evaluated by MTT assay

Complex	IC ₅₀ (μ M) ^a MCF	IC ₅₀ (μ M) ^a HeLa
Doxycycline	0.80 \pm 0.06	0.70 \pm 0.03
1	0.87 \pm 0.06	0.73 \pm 0.06
2	0.79 \pm 0.04	0.72 \pm 0.04
3	0.46 \pm 0.05	0.55 \pm 0.04
4	0.75 \pm 0.07	0.79 \pm 0.08

^a Results represent mean of three independent experiments.

IC₅₀ values of some widely studied antibiotics and their ternary Cu(II) complexes are presented in Table 7. The comparison of these revealed that mixed-ligand copper complexes of antibiotics exhibit enhanced cytotoxic effect than the parent antibiotic.

Table 7: IC₅₀ values of antibiotics and their ternary copper complexes against cancer cell lines

Compound	IC ₅₀ (μM) (cell line)	Reference
Moxifloxacin (MFL)*	1.4 (A549)	52
[Cu(MFL)(phen)].5H ₂ O*	0.1 (A549)	52
[Cu(MFL)(bpy)].5H ₂ O*	0.4 (A549)	52
[Cu(MFL)(bpy)Cl] (BF ₄)	16.7 ± 2.2 (MCF-7)	53
[Cu(MFL)(phen)Cl] (BF ₄)	18.1 ± 2.6 (MCF-7)	53
Gatifloxacin (GFL)*	1.3 (A549)	52
[Cu(GFL)(phen)].5H ₂ O*	0.1 (A549)	52
[Cu(GFL)(bpy)].5H ₂ O*	0.75 (A549)	52
[Cu(TMCPMP-TS)(Phen)]	0.24 (A549)	54
[Cu(TPMP)(phen)NCS]	>0.157 (A549)	55
[Cu(TPMP)(bpy)NCS]	>0.157 (A549)	55
[Cu(TPMP-BA) ₂]	0.157 (A549)	55
2-furoic acid hydrazide (hyd)	>400 (K562) ^a	56
[Cu(hyd)(bpy)(acn)(ClO ₄)](ClO ₄)	25.0 ± 2.4 (K562) ^a	56
[Cu(hyd)(phen)(acn)(ClO ₄)](ClO ₄)	2.2 ± 2.3 (K562) ^a	56
thiophenecarboxylic acid hydrazide (shyd)	>400 (K562) ^a	56
[Cu(shyd)(bpy)(acn)(ClO ₄)](ClO ₄)	20.7 ± 2.0 (K562) ^a	56
[Cu(shyd)(phen)(acn)(ClO ₄)](ClO ₄)	1.5 ± 0.2 (K562) ^a	56
Sparfloxacin (Hsf)	No cytotoxic effect (HL-60) ^b	57
[Cu(sf)(bpy)Cl]	100 (HL-60) ^b	57
[Cu(sf)(phen)Cl]	100 (HL-60) ^b	57
N-propyl-norfloxacin (Hpr-norf)	No cytotoxic effect (K562 and HL-60)	58
[Cu(pr-norf)(bpy)]	<10μg/ml (K562 and HL-60)	58
Doxycycline (DOX)	0.80 ± 0.06 (MCF-7) 0.70 ± 0.03 (HeLa)	Present work
[Cu(DOX)(bpy)(H ₂ O)](NO ₃)	0.87 ± 0.06 (MCF-7) 0.73 ± 0.06 (HeLa)	Present work
[Cu(DOX)(phen)(H ₂ O) ₂](NO ₃) ₂	0.79 ± 0.04 (MCF-7) 0.72 ± 0.04 (HeLa)	Present work
[Cu(DOX)(dpq)(H ₂ O) ₂](NO ₃) ₂	0.46 ± 0.05 (MCF-7) 0.55 ± 0.04 (HeLa)	Present work
[Cu(DOX)(dppz)(H ₂ O) ₂](NO ₃) ₂	0.75 ± 0.07 (MCF-7) 0.79 ± 0.08 (HeLa)	Present work

* IC₅₀ of MFL, GFL and their respective complexes are estimated from graph ^a after 72 h, ^b IC₅₀ in μg/ml, TMCPMP-TS=pyrazolone based thiosemicarbazone, TPMP=toluyalation of pyrazolone, bpy =bypyridine, phen=phenanthroline, dpq= dipyrido[3,2-d:2',3'-f]quinoxaline and dppz= dipyrido[3,2-a:2',3'-c]phenazine, acn =Acetonitrile

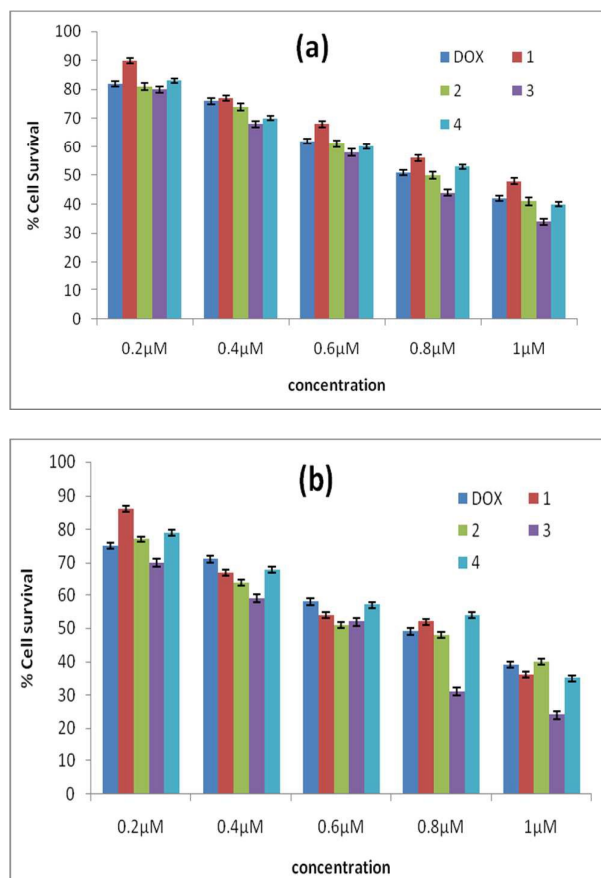


Figure 9. Cytotoxicity evaluation of doxycycline and 1-4 against MCF-7 and (b) HeLa cell lines. The cell viability was assessed after 48 h by the MTT assay. (The experiment is carried out in the triplicate under identical conditions)

Conclusions

The mixed-ligand copper (II) complexes of doxycycline with a series of diimine ligands have been synthesized and characterized. **1** exhibits square-pyramidal coordination geometry at the Cu(II) site, while **2** exhibits distorted octahedral coordination. The crystal structures of **1** and **2** are the first structures of coordinated doxycycline which unambiguously confirm that out of several binding sites, doxycycline coordinates through enolate oxygen of ring A in **1** and the diketoamide of ring A in **2**. All complexes cleave pBR322 DNA by oxidative mechanism at significantly low concentration. All complexes inhibit MMP-2 activity significantly, with **3** being the most potent, even better than the parent doxycycline ligand. Complexes are cytotoxic towards MCF-7 and HeLa cell lines with **3** exhibiting highest activity, which correlates well with MMP inhibition ability. These studies suggest that the mode of cell death effected by these complexes is probably MMP inhibition. Antimalarial activity of these complexes against the chloroquine-sensitive *Plasmodium falciparum* NF54 and chloroquine-resistant *Plasmodium falciparum* Dd2 strains reveal that complexes bear higher activity than Artesunate drug against chloroquine-resistant Dd2 strain.

Acknowledgements

OOA Acknowledges DBT-TWAS Postgraduate Fellowship (FR number: 3240240274). NAV acknowledge Department of Science and Technology, New Delhi for fellowship (SR/WOS-A/CS-63/2010). ASK and SBS acknowledge Department of Science and Technology (DST), New Delhi (SR/S1/IC-25/2010). We thank Dr. D. Srinivas, NCL, Pune for discussion on EPR. ASK acknowledge Royal Society of Chemistry for Journal Grant for International Authors and the kind hospitality of Dr. Andrea Erxleben, School of Chemistry, National University of Ireland, Galway, Ireland. The authors thank SAIF, CDRI, Lucknow, India for ESI-MS and elemental analyses and SAIF, IIT Bombay, India for EPR analysis. JAO is grateful for the support from the Science and Technology Education Post-Basic Project (STEP-B). PS and CdK acknowledge support from the South African Medical Research Council.

References

- M. O. Griffin, E. Fricovsky, G. Ceballos F. Villarreal, *Am. J. Physiol.* 2010, **35**, 3523.
- A. Bruke, M.D. Cunha, *Med. Clin. North Am.* 2006, **90**, 1089
- B. Yang, Y. Lu, A. Zhang, A. Zhou, L. Zhang, L. Zhang, L. Gao, Y. Zang, X. Tang, L. Sun *PLoS One.* 2015, **10**, 1-12
- J. F. Fisher, S. Mobashery, *Cancer Metastasis Rev.*, 2006, **25**, 115–136
- M. R. Acharya, J. Venitz, W. D. Figg, A. Sparreboom, *Drug Resist. Updat.*, 2004, **7**, 195–208
- C. Gialeli, A. D. Theocharis, N. K. Karamanos, *FEBS Journal*, 2011, **278**, 16–27
- R.S. Fife, G. W. Sledge, *J. Lab Clin. Med.*, 1995, **125**, 407–11
- M. Hidalgo, S. G. Eckhardt, *J. Natl. Cancer Inst.*, 2001, **93**, 178–193
- L. A. Di Nezza, A. Misajon, J. Zhang, T. Jobling, M.A. Quinn, A.G. Ostor, G. Nie, A. Lopata, L. A. Salamonsen, *Cancer*, 2002 **94**, 1466–1475
- M. Brion, G. Berthon, F. B. Fourtillan, *Inorg. Chim. Acta*, 1981, **55**, 47–56
- B. Zakeri, G. D. Wright, *Biochem. Cell. Biol.*, 2008, **86**, 124–136
- E. K. Efthimiadou, H. Thomadaki, Y. Sanakis, C. P. Raptopoulou, N. Katsaros, A. Scorilas, A. Karaliota G. Psomas *J. Inorg. Biochem.* 2007, **101**, 64–7
- F. Dimiza, S. Fountoulaki, A. N. Papadopoulos, C. A. Kontogiorgis, V. Tangoulis, C. P. Raptopoulou, V. Psycharis, T. Terzis, D. P. Kessissoglou, G. Psomas *Dalton Trans.*, 2011, **40**, 8555–8568
- P.P. Silva, W. Guerra, J. N. Silveira, A. M. d. C. Ferreira, T. Bortolotto, F. L. Fischer, H. Terenzi, A. Neves, E. C. Pereira-Maia, *Inorg. Chem.*, 2011, **50**, 6414–6424
- T. Bortolotto, P. P. Silva, A. Neves, E. C. Pereira-Maia, H. Terenzi, *Inorg. Chem.*, 2011, **50**, 10519–10521
- O. M. M. Santos, D. M. Silva, F. T. Martins, A. O. Legendre, L. C. Azarias, I. M. L. Rosa, P. P. Neves, M. D. de Araujo, A.C. Doriguetto, *Cryst. Growth Des.* 2014, **14**, 3711–3726
- O. Legendre, L. R. R. Silva, D.M. Silva, I.M.L. Rosa L. C. Azarias, P. J. de Abreu, M. B. de Araujo, P. P. Neves, Claudia Torres, C.; Martins, F.T.; Doriguetto, A.C. *Cryst Eng Comm*, 2012, **14**, 2532
- F. W. Heinemann, C. F. Leybold, C. R. Roman, M.O.Schmitt S. Schneider, *J. Chem Crystallogr* 2013, **43**, 213–222
- M. Yamada, Y. Tanaka, Y. Yoshimoto, S. Kuroda, I. Shima, *Bull. Chem. Soc. Jpn.*, 1992, **65**, 1006–1011
- J. G. Collins, A. D. Sleeman, J. R. Aldrich-Wright, L. Greguric, T. W. Hambley, *Inorg. Chem.*, 1998, **37**, 3133–3141
- J. E. Dickerson, L. A. Summers, *Aust. J. Chem.*, 1970, **23**, 1023–1027
- SHELXTL 2013*, Bruker AXS Inc. Madison, WI, 2013
- H. D. Flack, *Acta Crystallogr., Sect. A: Found. Crystallogr.*, 1983, **39**, 876–881
- G. M. Sheldrick, *Acta Crystallogr., Sect. A: Found. Crystallogr.*, 2008, **64**, 112–122
- G. M. Sheldrick, *SHELXTL-PLUS (VMS)*, Siemens Analytical X-ray Instruments, Inc. Madison, WI, 1990
- P. McArdle, K. Gilligan, D. Cunningham, R. Dark, M. Mahon, *CrystEngComm*, 2004, **6**, 303–309
- P. McArdle, *J. Appl. Crystallogr.*, 1995, **28**, 65 PC Windows version
- M. W. Roomi, J. C. Monterrey, T. Kalinovsky, M. Rath, Niedzwiecki, A.; *oncology reports* 2010, **23**, 605–614
- W. Trager, J.B. Jensen, *Science*, 1976, **193**, 673
- M. T. Makler, D. J. Hinrichs, *Am. J. Trop. Med. Hyg.*, 1993, **48**, 205
- A. Barve, A. Kumbhar, M. Bhat, B. Joshi, R. Butcher, U. Sonawane, R. Joshi, *Inorg. Chem.*, 2009, **48**, 9120–9132
- S. S. Bhat, A. A. Kumbhar, H. Heptullah H.; A. A. Khan, V. V. Gobre, S. P. Gejji, V.G. Puranik, *Inorg. Chem.*, 2011, **50**, 545–558
- M.V. Veidic, G. H. Schreiber, T. E. Gough, G. H. Palenik, *J. Am. Chem. Soc.*, 1969, **91**, 1859–1860
- C. R. Choudhury, S. K. Dey, S. Mitra, V. Gramlich, *Dalton Trans.*, 2003, 1059–1060
- P.C. Chieh, G. G. Messmer, G. J. Palenik, *Inorg. Chem.*, 1971, **10**, 133–138
- J. Dziegielewski, J. Hanuza, B. Jezowska-Trzebiatowska, *Bull. Acad. Pol. Sci., Ser. Sci. Chim.*, 1976, **24**, 307–322
- C. Rajarajeswari, R. Loganathan, M. Palaniandavar, E. Suresh, A. Riyasdeen, M. A. Akbarsha, *Dalton Trans.*, 2013, **42**, 8347–8363
- Y. An, M-L.Tong, L-N. Ji, M-W. Mao, *Dalton Trans.*, 2006, 2066–2071
- B. Selvakumar, V. Rajendiran, P.U. Maheswari, Stoeckli, H. Evans, M. Palaniandavar *J. Inorg. Biochem.*, 2006, **100**, 316–330
- A. R. Biju, M. V. Rajasekharan, S.S. Bhat, A. A. A.A. Khan, A. S. Kumbhar, *Inorg. Chem. Acta.*, 2014, **423**, 93–97
- M. V. Kech, S. J. Lippard, *J. Am. Chem. Soc.* 1992, **114**, 3386
- A. Vacca, M. Bruno, A. Boccarelli, M. Coluccia, D. Ribatti, A. Bergamo, S. Garbisa, L. Sartor, G. Sava, *Br. J. Cancer*, 2002, **86**, 993 – 998
- R. Sasanelli, A. Boccarelli, D. Giordano, M. Laforgia, F. Arnesano, G. Natile, C. Cardellicchio, M. A. M. Capozzi, M. Coluccia, *J. Med. Chem.*, 2007, **50**, 3434–3441
- F. Arnesano, A. Boccarelli, D. Cornacchia, F. Nushi, R. Sasanelli, M. Coluccia, G. Natile, *J. Med. Chem.*, 2009, **52**, 7847–7855
- A. Schröpfer, U. Kammerer, M. Kapp, J. Dietl, S. Feix, J. Anacker, *BMC Cancer* 2010, **10**, 553
- K. R. Tan, A. J. Magill, M. E. Parise, P. M. Arguin, *Am. J. Trop. Med. Hyg.*, 2011, **84**, 517–531
- M. Navarro, *Coord. Chem. Rev.*, 2009, **253**, 1619–1626.
- M. Navarro, C. Gabbiani, L. Messori, D. Gambino *Drug Discovery Today* 2010, **15**, 1070–1078
- N. I. Wenzel, N. Chavain, Y. Wang, W. Friebolin, L. Maes, B. Pradines, M. Lanzer, V. Yardley, R. Brun, C. Herold-Mende, C. Biot; K. Tóth, E. Davioud-Charvet, *J. Med. Chem.* 2010, **53**, 3214–3226
- C. S. K. Rajapakse, A. Martínez, B. Naoulou, A. A. Jarzecki, L. Suárez, C. Deregnacourt, V. Sinou, J. Schrével, E. Musi, G. Ambrosini, G. K. Schwartz, R. A. Sánchez-Delgado, *Inorg. Chem.*, 2009, **48**, 1122–1131

ARTICLE

Journal Name

- 51 C. Biot, W. Castro, C. Y. Bottéd, M. Navarro, *Dalton Trans.*, 2012, **41**, 6335-6349
- 52 R. Singh, R. N. Jadeja, M. C. Thounaojam, T. Patel, R. V. Devkar, D. Chakraborty, *Inorg. Chem. Commun.* 2012, **23**, 78-84
- 53 S. Patitungkho, S. Adsule, P. Dandawate, S. Padhye, A. Ahmad, F. H. Sarkar *Bioorg. Med. Chem. Lett.*, 2011, **21**, 1802-1806
- 54 K. M. Vyas, R. N. Jadeja, D. Patel, R.V. Devkar, V. K. Gupta *Polyhedron*, 2013, **65**, 262-274
- 55 K. M. Vyas, R. N. Jadeja, D. Patel, R.V. Devkar, V. K. Gupta, *Polyhedron* 2014, **80**, 20-33
- 56 P. P. Silva, W. Guerra, G. Coelho dos Santos, N. G. Fernandes, J. N. Silveira, A. M. da C. Ferreira, T. Bortolotto, H. Terenzi, A. J. Bortoluzzi, A. Neves, E. C. Pereira-Maia *J. Inorg. Biochem.*, 2014, **132**, 67-76
- 57 E. K. Efthimiadou, M. E. Katsarou, A. Karaliota, G. Psomas, *J. Inorg. Biochem.* 2008, **102**, 910-920
- 58 E. K. Efthimiadou, H. Thomadaki, Y. Sanakis, C. P. Raptopoulou, N. Katsaros, A. Scorilas, A. Karaliota, G. Psomas, *J. Inorg. Biochem.*, 2007, **101**, 64-73

